Building Simulation 2009

Eleventh International IBPSA Conference
Glasgow, Scotland
July 27-30, 2009

VALIDATION OF THE ZONAL METHOD FOR THE CASE OF ISOTHERMAL AIRFLOW IN A RECTANGULAR CAVITY

Tiago Czelusniak[1], Kátia Cordeiro Mendonça[1], Marc Olivier Abadie[1,2]
[1]Pontifical Catholic University of Parana – PUCPR
Curitiba – PR – 80215-901 – Brazil
[2]LEPTIAB – University of La Rochelle – 17000 La Rochelle – France

ABSTRACT

The objective of this work is to evaluate the quality of the predictions of the indoor airflow behaviour by the zonal method in comparison to the CFD results. The isothermal airflow of the International Energy Agency Annex 20 test cell was chosen to perform the proposed comparative analysis. This cell represents a rectangular room where the air is supplied horizontally on the upper left and is exhausted through an opening located on the lower right on the opposite side. Results are presented in terms of dimensionless mean velocity between zones considering different zonal grid schemes of the indoor environment.

INTRODUCTION

Air-conditioning systems are supposed to provide comfort and healthy indoor air conditions in confined spaces. However, these equipments can produce gradients of the psychrometric properties and, as a consequence, can:

- cause to occupants a sensation of discomfort even when their global thermal perceptions of the indoor environment remain satisfactory,
- expose the occupants differently to pollutants sources,
- affect the heat and mass transfers between the indoor environment and its envelope, and therefore the building energy consumption.

Thus, for accurately evaluating the energy consumption in conditioned buildings while maintaining acceptable thermal comfort and healthy conditions, it is important to take into account the indoor air distribution on the evaluation.

Nevertheless, as the computational fluid dynamics (CFD) is time consuming, the most common building simulation programs like ENERGYPLUS (Crawley et al., 2004), TRNSYS (Klein et al., 2004) and WUFI (Holm et al., 2003) make use of the global modelling, which does not consider any heterogeneity in the environment.

The heterogeneous behaviour of enclosed environments can be alternatively predicted by the zonal method. This methodology is an intermediate approach between the global modelling and the CFD. The classic zonal model approach uses a coarse spatial discretisation, in which the psychrometric conditions of the air in each control volume are considered uniform, except for pressure that varies hydrostatically. In this methodology only the mass and energy balance equations are solved for each control volume of the domain. The Navier-Stokes equations are replaced by a simplified version of the momentum equation and, hence, do not allow the description of the flow pattern promoted by mechanical ventilation. Empirical and semi-empirical equations are then added to the basic formulation in order to make it possible to predict the indoor air behaviour in conditioned spaces.

Although the zonal method has been used in a large number of applications in the last three decades (Megri and Haghighat, 2007), a completely validated model including the most common driving flows in buildings is still lacking.

In the context of spaces ventilated by a jet airflow issue of an air-conditioning system, a few works on the validation of the corresponding zonal model can be cited. The quality of predictions from the classic zonal approach combined to a 2D jet model (Musy, 1999; Mora et al., 2003; Galanis and Daoud, 2008) or a 3D jet model (Galanis and Daoud, 2008) were evaluated by confronting them against experimental data available in the current literature (Castanet, 1998; Nielsen, 1990). The experimental results concerned a square or a rectangular cell test ventilated by a horizontal wall jet. In those slightly different studies, the jet region was much better represented quantitatively than the recirculation zone of the room. However, it is important to remark that only a few number of experimental data were available, and also that some comparisons were performed in terms of velocity profiles although the zonal method can only give a mean value at the interface of each zone.

Therefore, the present study aims to contribute to the validation of the zonal models to simulate conditioned buildings, by comparing their predictions to the CFD results (that have been previously validated) for a specific study case. In a first part, a short description of the two models implemented in the zonal methodology is provided: the standard model used in the flow regions with weak momentum and the model needed to correctly

evaluate the air jet behaviour. In a second part, the studied geometry and the zonal partitioning principles are presented. Comparisons to CFD predictions are then given in a third part.

ZONAL MODEL DESCRIPTION

The mathematical model used in the description of the edification is composed of the two models according to Mendonça (2004): the "standard model" that represents the flow regions with weak momentum and the "air jet model" that describes the air behaviour in the jet region. The model regarding the envelope is not described here as the studied case does not present heat or moisture transfer through the envelope.

Standard model

In the standard model each zone is described by two sets of equations. The first one determines the physical characteristics of the indoor air, being made up by the conservations of mass and energy equations and by equations of state. The second one is composed of the equations that determine the heat and mass transfer between the zone and its neighbouring zones.

Assuming that the indoor air in a zone is well mixed, the mass conservation (dry air and water vapour) and the energy conservation equations can be expressed as follows:

$$\sum_{i=1}^{6} \dot{m}_{da} = 0 \tag{1}$$

$$V \frac{d\rho_{wv}}{d\tau} = \sum_{i=1}^{6} \dot{m}_{wv} + \dot{m}_{wv,source} \tag{2}$$

$$\rho_{da} c_{p\,da} V \frac{dT_{ma}}{d\tau} = \dot{q}_{source} + \sum_{i=1}^{6} \dot{Q} \tag{3}$$

The index i refers to one of the six faces of the zone. Note in Eq. (1) that the temporal variation of dry air mass inside the zone has been neglected.

The thermodynamical properties of indoor air are related to each other by the ideal gas equation, equation (4), and by psychrometric relations expressed in equations (5) to (7).

$$P_{\mathrm{ma}} = \left(\rho_{\mathrm{da}} \Re_{\mathrm{da}} + \rho_{\mathrm{wv}} \Re_{\mathrm{wv}}\right) T_{\mathrm{ma}} \tag{4}$$

$$\rho_{\mathrm{ma}} = \rho_{\mathrm{da}} + \rho_{\mathrm{wv}} \tag{5}$$

$$w = \rho_{wv} / \rho_{da} \tag{6}$$

$$\varphi = \left(\rho_{wv} \Re_{wv} T_{ma} / P_{wv,sat}\right)_{P_{ma}, T_{ma}} \tag{7}$$

An additional equation is used to evaluate the saturation pressure of water vapor of equation (7). In this study, the expression proposed by Woloszyn (1999) was adopted.

The evaluation of the dry air mass flow rate between two neighbouring zones is based on the orifice flow equation. In this approach, this flow is calculated differently for vertical and horizontal interfaces because hydrostatic effects are taken into account in the latter. For vertical interfaces the dry-air mass flow rate can be calculated as follows:

If $p_{\mathrm{ma},1} - p_{\mathrm{ma},2} \geq 0$ then

$$\dot{m}_{\mathrm{da}} = C_d A \rho_{\mathrm{da},1} \sqrt{2\left(p_{\mathrm{ma},1} - p_{\mathrm{ma},2}\right) / \rho_{\mathrm{ma},1}} \tag{8a}$$

else

$$\dot{m}_{\mathrm{da}} = -C_d A \rho_{\mathrm{da},2} \sqrt{2\left(p_{\mathrm{ma},2} - p_{\mathrm{ma},1}\right) / \rho_{\mathrm{ma},2}} \tag{8b}$$

The indices 1 and 2 correspond, respectively, to the left and right zone separated by the vertical interface.

The same equations can be used in the case of a horizontal interface, except that in this case the pressure at the interface ($\mathrm{p}^{*}_{\mathrm{ma}}$) depends on zone dimensions:

$$\mathrm{p}^{*}_{\mathrm{ma},1} = p_{\mathrm{ma},1} + \rho_{\mathrm{ma},1} \mathrm{g}\left(\mathrm{h}_1 / 2\right) \tag{9a}$$

$$\mathrm{p}^{*}_{\mathrm{ma},2} = p_{\mathrm{ma},2} - \rho_{\mathrm{ma},2} \mathrm{g}\left(\mathrm{h}_2 / 2\right) \tag{9b}$$

where the indices 1 and 2 correspond, respectively, to the zone above and below the interface.

The mass flow rate of water vapor is composed by two terms: one diffusive and other due to the difference of pressure between neighbouring zones. The mass flow rate of water vapor caused by the difference of pressure is based on the mass flow rate of dry air, as given by equations (10a) and (10b).

If $p_{\mathrm{ma},1} - p_{\mathrm{ma},2} \geq 0$ then

$$\dot{m}_{\mathrm{wv}} = \rho_{\mathrm{wv},1} \left(\dot{m}_{\mathrm{da}} / \rho_{\mathrm{da},1}\right) \tag{10a}$$

else

$$\dot{m}_{\mathrm{wv}} = \rho_{\mathrm{wv},2} \left(\dot{m}_{\mathrm{da}} / \rho_{\mathrm{da},2}\right) \tag{10b}$$

The diffusive term is evaluated following Fick's law, given by equation (11).

$$\dot{m}_{wv} = D_{wv} A \left(\frac{\rho_1 + \rho_2}{2}\right) \left[\frac{\rho_{wv,1}/\rho_1 - \rho_{wv,2}/\rho_2}{\left(l_1 + l_2\right)/2}\right] \tag{11}$$

The heat transfer across an interface is described only by an advective term since the conductive flux is negligible compared to the first one. This advective flux is calculated by equations (12a) and (12b),

If $\dot{m}_{\mathrm{da}} \geq 0$ then

$$\dot{Q} = \dot{m}_{da} c_{p\,da} T_1 \tag{12a}$$

else

$$\dot{Q} = \dot{m}_{da} c_{p\,da} T_2 \tag{12b}$$

Air jet model

The jet cells are described by two sub-cells, one composed by specific equations of the jet, and the other described by the standard model. The same decomposition is applied to the jet interfaces, tangential and perpendicular to the flow.

The sub-cell that describes the behaviour of the horizontal jet is similar to the standard cell i.e., in this sub-cell, all the air properties are considered

constant, except for the pressure which varies hydrostatically. Hence, the mass and energy conservation equations for the jet are the same as for standard cell.

Because the standard model is described by a simplified momentum equation, it cannot represent correctly the airflow in the jet region. Thus, the simplified momentum equation is replaced by an empirical formulation, which in the context of this work corresponds to that for an isothermal two-dimensional jet (Abramovich, 1963; Rajaratman, 1976). In this air jet sub-cell, the mass flow rate at any distance of the inlet is then given by:

$$\dot{m}_{da} = \dot{m}_{da,inlet}\left(1 + 0.248\sqrt{\frac{x}{h}}\right) \quad (13)$$

It is assumed that the jet does not develop laterally as it flows, although mass flow rates will be induced from the lateral and frontal surfaces of the jet.

In order to represent the horizontal jet using the zonal approach, two parameters must be defined to enable the partitioning of the indoor environment: the jet throw and the maximum jet thickness.

The thickness of a horizontal plane jet at a distance x from the air supply diffuser is represented in figure 1.

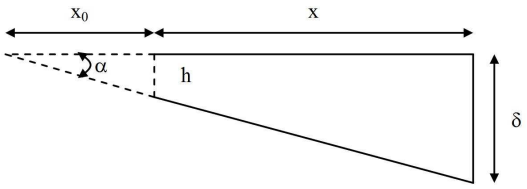

Figure 1 Representation of the jet expansion from its fictitious origin.

From the jet velocity profile for an isothermal two-dimensional jet (Abramovich, 1963; Rajaratman, 1976), this thickness can be expressed by equation (14) supposing the air velocity in the jet envelope is equal to 1% of the maximum one,

$$\delta = 2K_e x\sqrt{\frac{-\ln 0.01}{\ln 2}} \quad (14)$$

In the case of the jet throw, it can also be obtained from the jet velocity profile for an isothermal two-dimensional jet (Abramovich, 1963; Rajaratman, 1976), considering the maximum jet velocity equal to 0,25 m/s (ASHRAE, 2005), as expressed by equation (15).

$$x_{throw} = h\left(\frac{K_v U_{inlet}}{0.25}\right)^2 - x_0 \quad (15)$$

It must be remarked though that the constants K_e e K_v employed in this study correspond to those from Rajaratman (1976) for an isothermal linear wall jet.

The distance between the jet fictitious origin and the air diffuser (x_0) is evaluated using trigonometric relations and the jet angle value of 22°, commonly encountered in real configuration (ASHRAE, 2005).

METHODOLOGY

To study the jet's airflow, the zonal model was applied to the isothermal test case of Annex 20, described by Nielsen (1990). This case represents a room where the air is supplied horizontally on the upper left corner and is exhausted through the opening located on the lower right corner on the opposite side. Figure 2 shows a sketch of the room along with its dimensions: L=9.0m, W=3.0m, H=3.0m, h=0.168 m and t=0.48m. In the present study the inlet opening width is half that of the room i.e. v=1.5m.

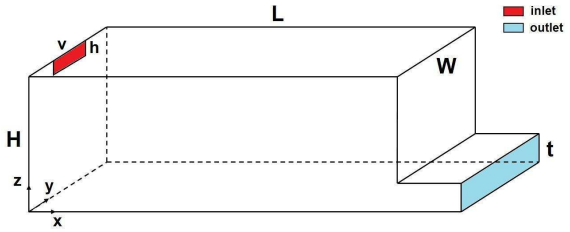

Figure 2 Sketch of the three-dimensional test case.

The inlet conditions for the velocity were specified as $U=U_0=0.455$m/s, corresponding to an inlet height-based Reynolds number of 5,000. Zero relative pressure was applied to the room's outlet. At the solid boundaries, the adiabatic and impermeable wall boundary conditions were specified.

As mentioned above, the zonal partitioning depends on thickness and the throw of the jet, described by equations (14) and (15), respectively. Solving equation (15) for the specified inlet conditions, the jet throw is x_{throw}=6.6m. Replacing x by x_{throw} in equation (14), the maximal jet thickness found is δ_{throw}=2.3m. This last dimension imposes the height of the upper layer of cells that has to be greater than the maximal jet thickness (see figure 3). The height of the lower layer of cells was taken equal to the outlet height. For the present case, only one intermediate horizontal layer, located between the lower and upper ones, has been used because of the remaining space of 0.22m. Note that the lower layer of cells could be higher than the outlet height, and the intermediate layer could have been therefore omitted without drastically modifying the results. It has been chosen to keep this layer, as this one would appear in most other configurations.

Based on this vertical distribution, three different horizontal partitionings have been applied to the study case by only modifying the number of cells in the jet zone as the treatment of the jet entrainment region can be regarded as the most critical part of the airflow. Hence, the number of cells in the jet region

has been increased from three to five cells. To finish, the number of cells in the last direction (along the y-axis of figure 2) has been fixed to three for all cases, with one central layer based on the inlet width (v) and two other lateral ones.

These three partitionings will be referenced in the next sections according to the total number of layers in each direction (xyz) i.e. zonal_433, zonal_533 and zonal_633.

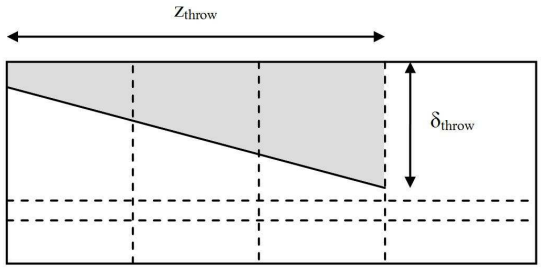

Figure 3 Zonal partitioning of the room – zonal_433.

The zonal library was developed into the modular simulation platform SPARK (Sowell and Haves, 2001). The simulations were made considering the Newton-Raphson component solving method and a Gaussian elimination matrix solving method, with a time step of 1s and a tolerance of 10^{-5}. The simulations were performed until steady state was achieved.

RESULTS AND ANALYSIS

In this section, the zonal results are compared to the CFD ones presented in Susin *et al.* (2009). The chosen CFD results have been obtained with the standard k-ε model (Laudner and Spalding, 1974) that demonstrated the best performance of the three tested turbulence models.

Airflow

Figure 4 upper graph presents the airflow field obtained using the standard k-ε model. More precisely, this graph shows the velocity vectors in the symmetry plane of the room (y=1.5m, figure 2). Four regions are clearly identified: the air jet zone with high horizontal positive velocities, the entrainment zone under the jet zone with essentially upward velocities, the zone of recirculation close to the outlet wall and the lower zone next to the floor with small horizontal negative velocities.

The lower graph of figure 4 presents the mean velocity across the interfaces between the zonal cells i.e. the mass flow rate divided by the interface areas. Consequently, the two graphs do not present exactly the same information: the first one gives the velocity at numerous points located in the symmetry plane of the room whereas the second one presents the mean velocity at cells interfaces of different heights and equal widths (=1.5 m). As a result, comparisons have to be made with caution. In the present case, the airflow is almost two-dimensional in the central region (along the y-axis) so the zonal velocity can be viewed as the average of the CFD velocity along the considered interface.

On the whole, the zonal method represents correctly the studied airflow. The air jet and lower zones are acceptably predicted. In particular, the dimensionless velocities are almost identical. The same observation can be made about the outlet velocity. The recirculation zone is completely included in the rightmost vertical cells layer so that it does not appears directly in the zonal representation. The main drawback seems to be linked to the air jet model. In particular, the jet width appears much larger in the zonal approach. The zonal representation shows also incorrect downward velocity between the jet and entrainment zones; this is partially compensated by a higher upward velocity (air flux) in the first jet cell, close to the air inlet.

Velocity Profiles at the interfaces

The objective of the zonal method is to evaluate the air mass fluxes between a reduced amount of cells and does not aim to have a complete and accurate description of the airflow such as the CFD methodology. Nevertheless, the evaluation of those fluxes has to be precise enough to predict the convective transport of temperature, moisture and pollutants. In this section, the dimensionless mean velocity profiles (equivalent to the air mass flux in the present isothermal problem) at the interfaces between the cells obtained by the zonal and CFD methods are compared. Figures 5, 6 and 7 present the comparison between the CFD and the zonal_433, the zonal_533 and the zonal_633 results, respectively. Note that only the horizontal velocity profiles have been studied here for which comparisons between CFD and experimental results have shown good predictions of the numerical approach (Susin *et al.*, 2009).

Overall, the zonal profiles are close to the CFD ones. The directions of the air flux are correctly described by the zonal method with only one exception for the zonal_533 configuration (x=1.1H) where a slightly positive velocity is obtained instead of a small negative one. The main difference lies in the air jet zone where the jet thickness tends to be overestimated by the zonal method. Outside of the air jet zone, the grid refinement tends to improve slightly the zonal results. Such improvement can be observed comparing the lower parts of the profiles at x=1.33H for zonal_433 and at x=1.32H for zonal_533. It is also observed that the zonal predictions regarding the last interfaces (x=2.2H) are not modified despite of the modification of the partitioning in the first part of the room. In fact, this part of the room strongly depends on the jet behaviour whose thickness and velocity are independent of the zonal partitioning. Therefore, refining the zonal partitioning in the first section of the room has no impact on this region.

This illustrates one important fundamental difference between the CFD and zonal methodologies.

CONCLUSION

The objective of this study was to evaluate the quality of the predictions of the indoor airflow obtained by the zonal method in the case of a room presenting an isothermal horizontal jet close to the ceiling.

In general, the zonal results presented here are comparable to those obtained with the CFD methodology. The main difference concerns the entrainment zone under the air jet where the observed discrepancies are probably consequences of the air jet model implemented for this analysis. In particular, even if this air jet model predicts correctly the air mass flow, it largely overestimates the jet thickness. The present work also illustrates the basic rules of zonal partitioning and the effect of the refinement that can modify the predictions in some regions (where the influence of the air jet model is weak) while letting unchanged other ones.

The present study is the first step of a systematic, rigorous, validation of the zonal method. The next steps of the validation are:

- testing of other air jet models to improve the calculation of the air jet thickness,
- comparison of the vertical air mass flux between the cells with the CFD predictions,
- analysis of the complete three-dimensional problem integrating a three-dimensional air jet model,
- validation of anisothermal-related problems, and
- investigation of the zonal method quality for different room geometries (cubical ones and atrium).

ACKNOWLEDGEMENT

The authors would like to acknowledge the CNPq (Brazilian Research Council), as well as *Fundação Araucária* for supporting this work.

REFERENCES

Abramovich, G.N. 1963. The theory of turbulent jets, MIT press, Cambridge, USA.

ASHRAE. 2005. ASHRAE Handbook of Fundamentals. American Society of Heating, Refrigerating and Air-Conditioning Engineers, Inc.

Castanet, S. 1998. Contribution à l'étude de la ventilation et de la qualité de l'air des locaux, Ph.D. Thesis, INSA de Lyon, France. (in French).

Crawley, D.B., Lawrie, L.K., Pedersen, C.O., Winkelmann, F.C., Witte, M.J., Strand, R.K., Liesen, R.J., Buhl, W.F., Huang, Y.J., Henninger, R.H., Glazer, J., Fisher, D.E., Shirey Iii, D.B., Griffith, B.T., Ellis, P.G., Gu, L. 2004. EnergyPlus: An Update, Proceedings of the SimBuild 2004 Conference, Boulder, Colorado.

Daoud, A., Galanis N. 2008. Predictions of airflow patterns in a ventilated enclosure with zonal methods, Applied energy, 85 (6) , pp. 439-448.

Holm, A., Kuenzel, H.M., Sedbauer, K. 2003. The Hygrothermal Behaviour of Rooms: Combining Thermal Building Simulation and Hygrothermal Envelope Calculation. Proceedings of the 8th International IBPSA Conference, Eindhoven, The Netherlands.

Klein S. A., Beckman W.A., Mitchell, J.W., Duffie, J.A., Duffie, N.A., Freeman, T.L., Mitchell, J.C., Brau, J.E., Evans, B.L., Kummer, J.P., Urban, R.E., Fiksel, A., Thornton, J.W., Blair, N.J., Williams, P.M., Bradley, D.E., Mcdowell, T.P., Kummert, M. 2004. TRNSYS 16 – A TRaNsient System Simulation program, User manual, SEL, University of Wisconsin, Madison USA.

Laudner, B.E., Spalding, D.B. 1974. The numerical computation of turbulent flows, Comp. Meth. Appl. Mech. Energy, 100, pp. 291-298.

Nielsen, P.V. 1990. Specification of a two-dimensional test case, Technical Report, International Energy Agency, Annex 20, Air flow pattern within buildings.

Megri, A.C., Haghighat, F. 2007. Zonal modeling for simulating indoor environment of buildings: review, recent developments, applications, HVAC&R Research, 13 (6), pp. 48-66.

Mendonça, K.C. 2004. Modélisation thermo-hydro-aéraulique des locaux climatisé selon l´approche zonale: Prise en compte des phénomènes de sorption d´humidité, Ph.D. Thesis, Université de La Rochelle, France. (in French).

Mora, L., Gagdil, A.J., Wurtz, E. 2003. Comparing zonal and CFD model predictions of isothermal indoor airflows to experimental data, Indoor air, 13, pp. 77-88.

Musy, M. 1999. Génération automatique des modèles zonaux pour l'étude du comportement thermo-aéraulique des bâtiments, Ph.D. Thesis, Université de La Rochelle, France (in French).

Rajaratnam, N. 1976. Turbulent Jets, Elsevier Scientific Publishing Company, Amsterdam, The Netherlands.

Sowell, E. F., Haves, P. 2001. Efficient solution strategies for building energy system simulation, Energy and Buildings, 33, pp. 309-319.

Susin, R.M., Lindner, G.A., Mariani, V.C., Mendonça, K.C. 2009. Evaluating the influence of the width of inlet slot on the prediction of indoor airflow: Comparison with experimental

data, Building and Environment, 44 (5), pp. 971-986.

Woloszyn M. 1999. Modélisation hygro-thermo-aéraulique des bâtiments multizones: proposition d'une stratégie de résolution du système couple, Ph.D thesis, INSA de Lyon, France (in French).

NOMENCLATURE

A	Area	m^2
c_p	Specific heat	J/kg.K
C_d	Discharge coefficient	-
D	Diffusion coefficient	m/s
g	gravitational acceleration	m/s^2
h	Inlet height or height of the zone	m
H	Height of the room	m
K_e	Empirical constant (=0.068)	-
K_v	Empirical constant (=3.5)	-
L	Length of the room	m
l	Dimension perpendicular to the section of area A	m
$\dot{m}$	Mass flow rate	kg/s
p	Relative pressure of the zone	Pa
P	Total pressure	Pa
$\dot{q}$	Sensible heat	W
$\dot{Q}$	Time rate of heat transfer transported by air mass flow	W
$\mathcal{R}$	gas constant	J/kg.K
t	Outlet height	m
T	Temperature	K
U	Velocity component in x direction	m/s
V	Volume	m^3
w	Humidity ratio	kg/kg
W	Width of the room	m
x	Distance from the air inlet	m
x_0	Distance between the jet fictitious origin and the air diffuser	m

Greeks

α	Jet angle (=22°)	°
δ	Jet thickness	m
φ	Relative humidity	-
ρ	Density	kg/m^3
τ	Time	s

Subscripts

da	Dry air
wv	Water vapour
ma	Moist air
inlet	Inlet
sat	saturation
throw	Jet throw
source	Source

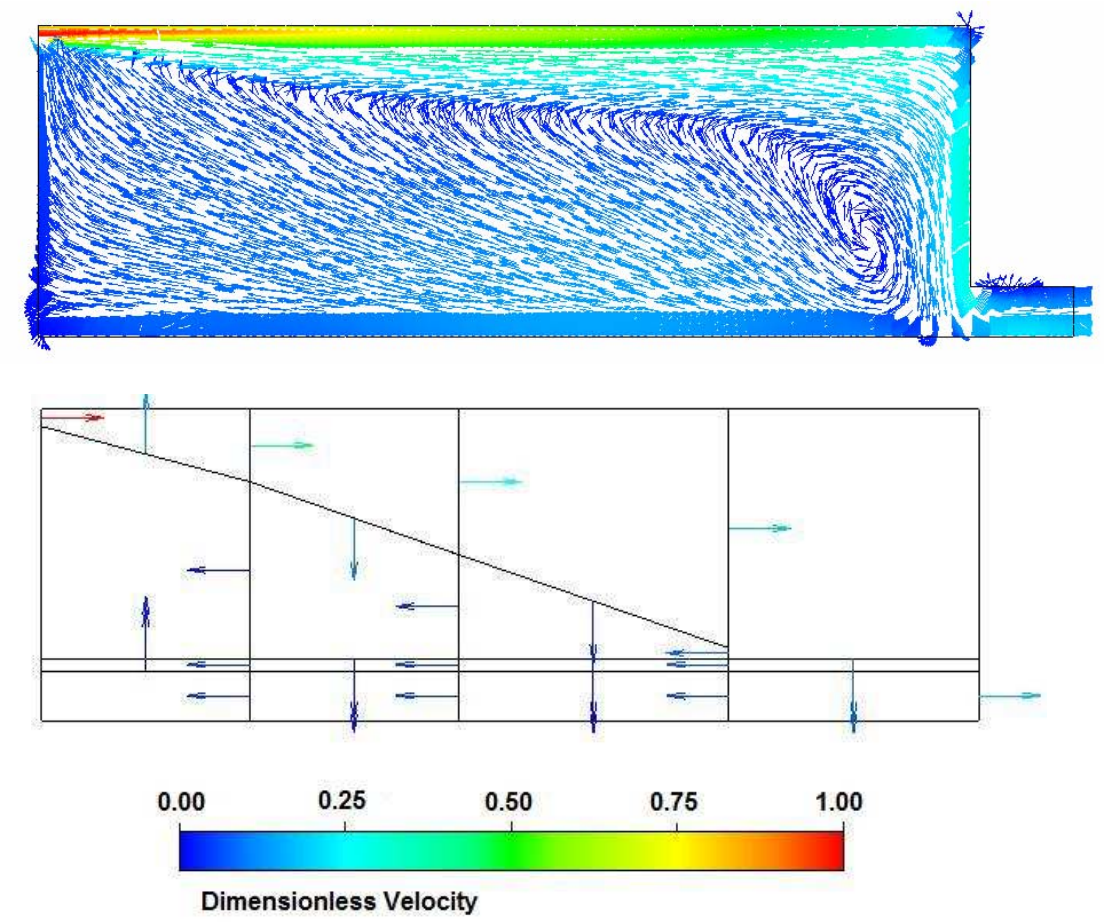

Figure 4 Airflow in the symmetry plane – upper graph: CFD, lower graph: zonal_433.

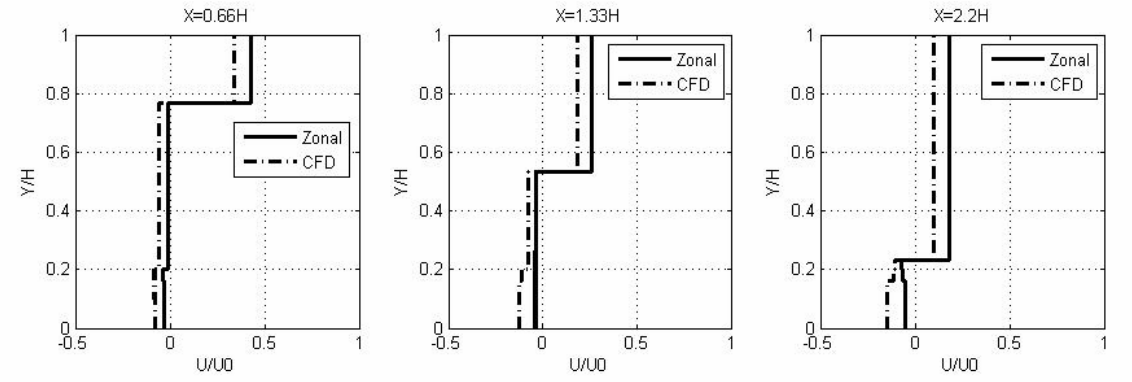

Figure 5 Dimensionless horizontal velocity profiles – comparison between zonal_433 and CFD.

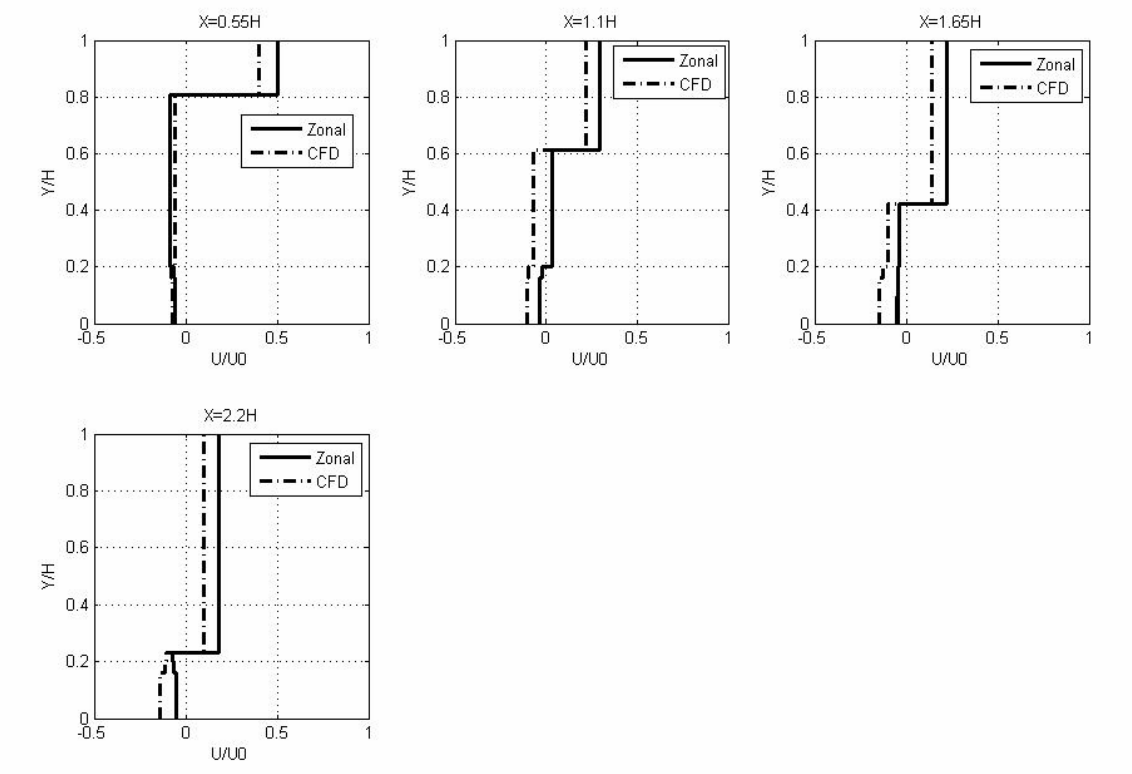

Figure 6 Dimensionless horizontal velocity profiles – comparison between zonal_533 and CFD.

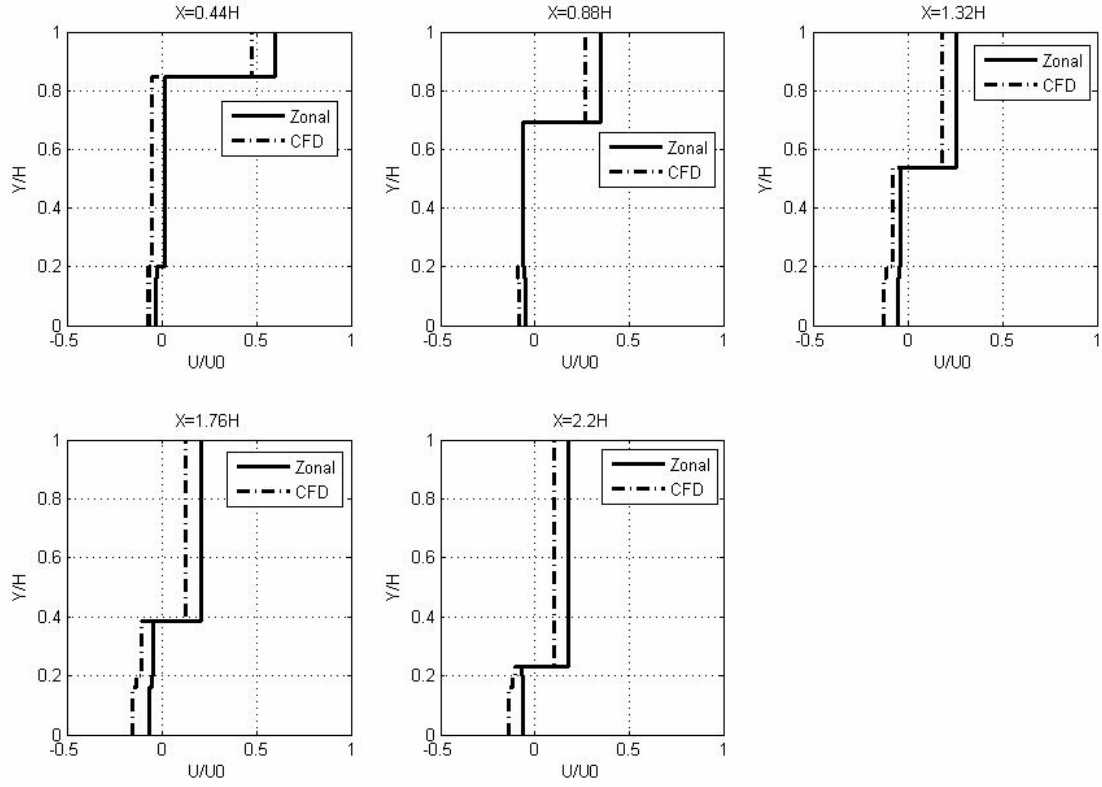

Figure 7 Dimensionless horizontal velocity profiles – comparison between zonal_633 and CFD.